To the Graduate Council:

I am submitting herewith a thesis written by Samuel C. Rogers entitled "Invention of a Tunable Damper for use with an Acoustic Waveguide in Hostile Environments." I have examined the final copy of this thesis for form and content and recommend that it be accepted in partial fulfillment of the requirements for the degree of Master of Science, with a major in Electrical Engineering.

J. M. Googe

J. M. Googe, Major Professor

We have read this thesis and recommend its acceptance:

R. W. Rochelle

Accepted for the Council:

C. W. Minkel

The Graduate School

INVENTION OF A TUNABLE DAMPER FOR USE WITH AN ACOUSTIC WAVEGUIDE IN HOSTILE ENVIRONMENTS

A Thesis

Presented for the

Master of Science

Degree

The University of Tennessee, Knoxville

Samuel C. Rogers

December 1983

ACKNOWLEDGEMENTS

The author gratefully acknowledges the guidance and encouragement of his Graduate Committee: Drs. J. M. Googe (Chairman), R. W. Rochelle, and J. C. Hung.

Special appreciation is given to the Instrumentation and Controls Division of the Oak Ridge National Laboratory, operated by the Nuclear Division of Union Carbide Corporation for the United States Department of Energy, for supplying the support necessary for the completion of this effort.

Appreciation is also expressed to the United States Nuclear Regulatory Commission Office of Nuclear Regulatory Research for sponsoring the research which led to this invention.

Recognition is given to R. L. Anderson, W. B. Dress, and G. N. Miller, all of the Instrumentation and Controls Division, for their technical contributions to the development of the acoustic waveguide for which the damper was invented.

Final thanks go to Robin O'Hatnick of the Information Processing Center, and Leon Smith of the Graphic Arts Department for their assistance in preparing this document.

ABSTRACT

A damper was invented to remove undesirable stress pulses from an acoustic waveguide. The damper was designed to be tunable, and constructed to withstand a corrosive or otherwise hostile environment. It serves to simplify the design and enhance the performance of a water level measurement system, of which the damper and acoustic waveguide are integral parts.

An experimental damper was constructed and applied to an existing level probe and measurement system. The resulting damper, properly tuned, causes acoustic stress pulses which pass into it along the waveguide to be completely attenuated.

TABLE OF CONTENTS

LIST OF FIGURES

FIGURE PAGE

CHAPTER I

INTRODUCTION

This thesis describes the invention of a tunable damper for use with an acoustic waveguide in hostile environments. The damper is a by-product of the research sponsored by the United States Nuclear Regulatory Commission, Division of Reactor Safety Research, which issued requirements for the development of improved instrumentation for use in pressurized water reactors to provide an unambigious indication of the adequacy of core cooling. Motivation for this effort stems from the analysis of the accident at the Three Mile Island Nuclear Power Plant, during which a condition of low water level and inadequate core cooling was not recognized for an extended period of time because no direct indication of water level in the reactor vessel existed.[1] The research was conducted at the Oak Ridge National Laboratory, which is operated by Union Carbide Corporation for the United States Department of Energy.

One such recent activity to satisfy the aforementioned requirements has been the development of an ultrasonic sensor and measurement system to determine the level of the fluid in which the sensor is immersed; specifically, the water level in a nuclear reactor vessel.[2] A simplified view of a nuclear reactor with the level measurement system in place is shown in Figure 1. This instrument, which will be described in Chapter II, depends on the reliable detection and precise time interval measurement of traveling acoustic waves that are introduced into and propagate along the length of an acoustic waveguide.

ORNL-DWG 83-1744C

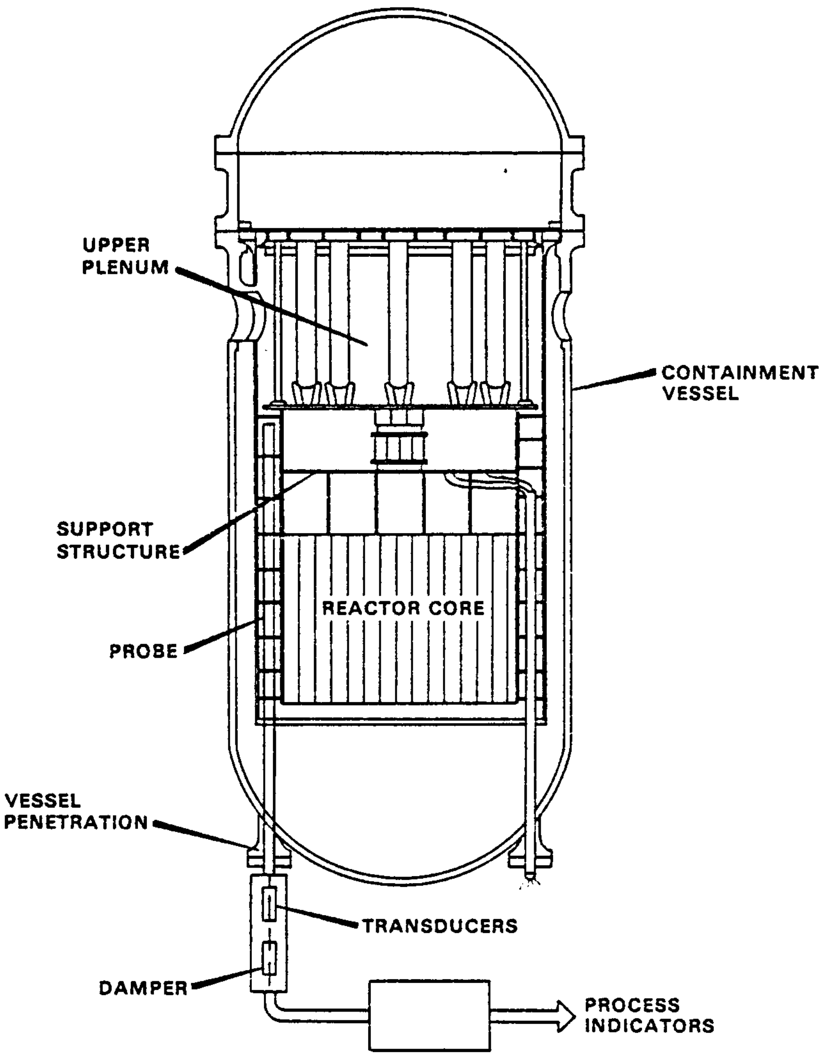

Figure 1. Ultrasonic level measurement system installed in reactor vessel.

When the acoustic waves are launched into the waveguide, they propagate in both directions along the waveguide (see Figure 2). The waves traveling in the back-length portion of the waveguide cannot be distinguished from reflected waves of interest returning from the sensing end of the waveguide without special considerations. In the original level sensor design, these undesirable back-end reflected waves were dealt with by utilizing a long back-length region and providing electronic sensing which only received echo pulses within predetermined time windows for echo pulse discrimination. This procedure was found to be unreliable and complicated the design of a sensor for reactor applications.

Therefore, an acoustic damper was designed to remove acoustic wave energy that enters the back-length section of the ultrasonic sensor (acoustic waveguide), and thereby simplify the design and improve the performance of the instrument. Under normal operating conditions, an instrument located inside a reactor vessel would be exposed to temperatures up to 375°C, pressures to 15.2 MPa, flowing water to 20 m/s, and intense nuclear radiation fields. Whereas conventional damper materials such as silicon rubber coating compounds, fiberglass insulation, etc., would not withstand a hostile environment such as that of a nuclear reactor, the subject damper is constructed entirely of stainless steel and, thus, is corrosion and radiation resistant.[3] Furthermore, the damper may be tuned to selectively absorb a given acoustic wave transmission mode and/or frequency, while allowing others to pass.

An experimental damper was constructed and applied to an existing level probe and measurement system. Tests were conducted in which

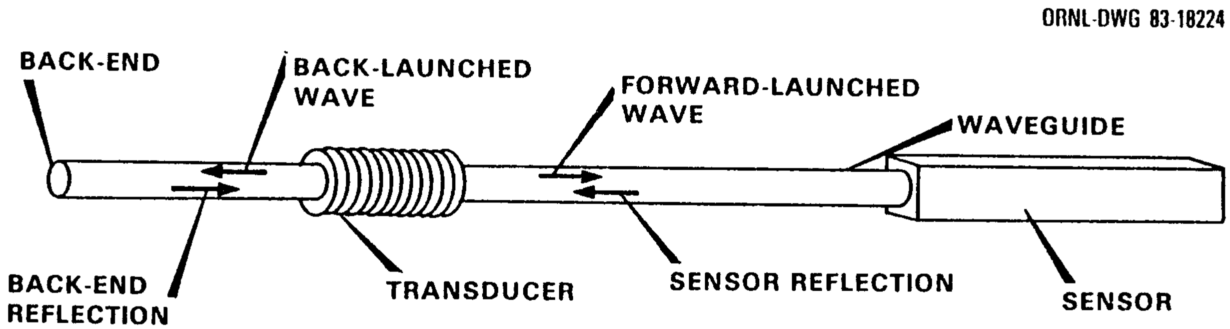

Figure 2. Acoustic waves launched in both directions along waveguide.

acoustic waves of different modes were passed into the damper along the waveguide, and the damper tuned until these waves were extinguished. A distributed parameter system model was subsequently developed to mathematically describe the damper's characteristics.

The following chapters are organized to generally follow the development sequence of the acoustic damper. Chapter II is a brief sketch of the background theory concerning the transduction and propagation of acoustic waves in thin waveguides, and a general description of the principle operation of the ultrasonic sensor and measurement system. Chapter III presents a detailed design and intuitive explanation of the damper mechanism, and then develops a mathematical model based on a distributed parameter analogy. Experimental procedures and results are provided in Chapter IV, followed by a summary in Chapter V.

CHAPTER II

DESCRIPTION OF MEASUREMENT SYSTEM

The principles of magnetostrictive generation and propagation of extensional and torsional acoustic stress pulses in thin waveguides are well known, and will be only briefly described here as a basis for further discussion concerning their application. The operation of the ultrasonic level measurement system is based on the principle that the propagation of torsional acoustic waves in a waveguide of noncircular cross-section is retarded by the fluid surrounding the waveguide. Consequently, the round-trip transit time of an acoustic wave traveling in the waveguide may be analyzed to yield the density (or level, if the density is known) of the fluid in which the waveguide is immersed. This chapter deals with the theory underlying the transduction and propagation of acoustic waves in thin waveguides, and describes the general operation of the level measurement system.

Background Theory

Extensional stress pulses (acoustic waves) and torsional stress pulses may be generated in magnetostrictive materials by utilizing the Joule and Wiedemann effects, respectively. A current pulse introduced into a coil surrounding a ferromagnetic rod creates a magnetic flux transient in the rod which causes a change in its length by the Joule effect (see Figure 3).[4] This sudden change in length produces an acoustic stress pulse which propagates as an extensional wave at the speed of sound within the material. Conversely, a returning extensional stress pulse passing under the coil produces a local dimensional

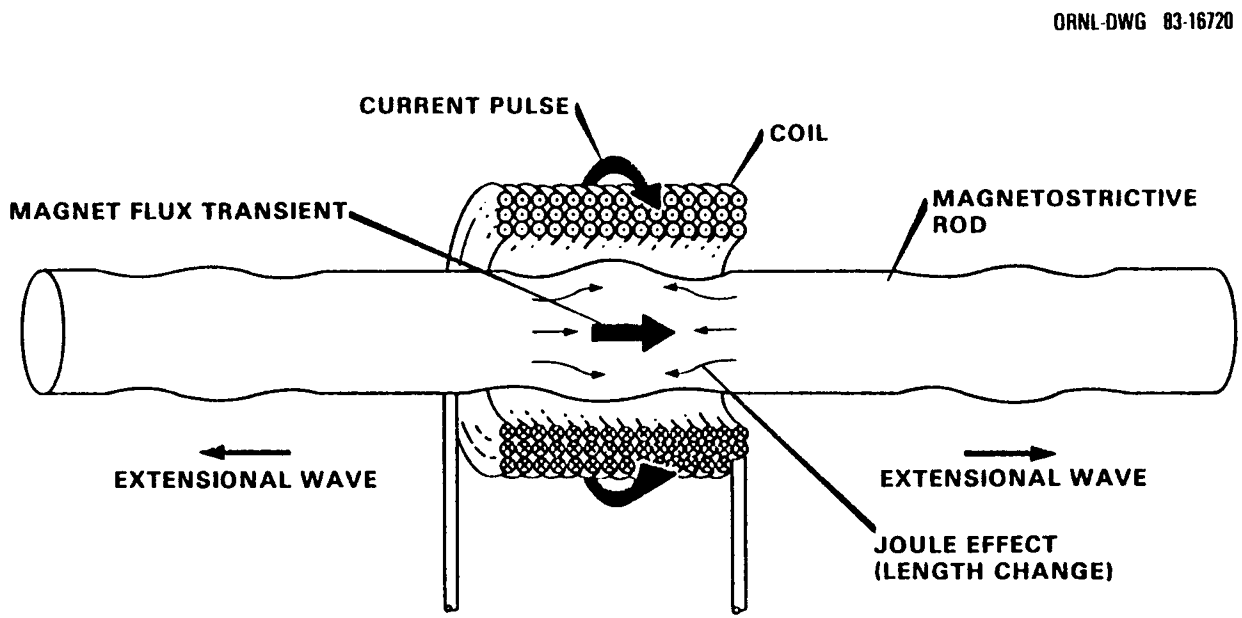

Figure 3. Generation of extensional waves in magnetostrictive rod by the Joule effect.

change which generates a change in flux that links the coil. This change in flux produces a voltage across the coil as a result of Faraday's law.

The Wiedemann effect, or torsional magnetostriction, is a two-dimensional extension of the Joule effect (see Figure 4).[5] A torsional stress pulse is produced in a magnetostrictive rod when a current pulse is applied to a coil surrounding the rod, causing a magnetic flux transient to interact with an azimuthal magnetic field existing in the rod. Such an azimuthal magnetic bias may be established in the rod by passing a dc current through the rod. The vector sum of the axially changing flux and the azimuthal bias produces a helical field that twists the rod and initiates a shear stress pulse in the rod. This shear stress pulse propagates as a torsional wave which, on its return to the coil, produces an output voltage across the coil by the inverse Wiedemann effect and Faraday's law.

In thin, elastic waveguides, acoustic stress pulses propagate as waves with a phase velocity proportional to the square root of a restoring force, or stiffness term (described by the elastic constants) divided by an inertia term (density or moment of inertia):

$$v = \sqrt{\frac{\text{stiffness term}}{\text{inertia term}}} \; . \qquad (1)$$

For a waveguide of noncircular cross-section, in a vacuum, the velocity of a dispersionless extensional wave and dispersionless torsional wave is expressed by

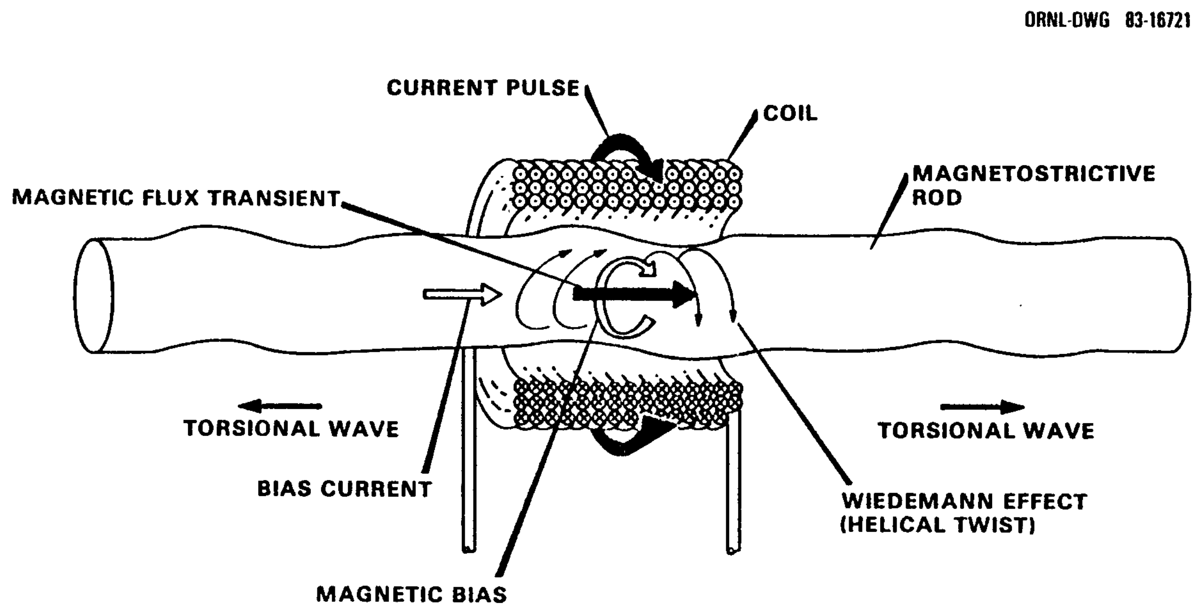

Figure 4. Generation of torsional waves in magnetostrictive rod by the Wiedemann effect.

$$v_e = \sqrt{\frac{Y}{\rho_w}} , \quad (2)$$

and,

$$v_t = K \sqrt{\frac{S}{\rho_w}} , \quad (3)$$

respectively. Young's modulus, Y, and the shear modulus, S, constitute the stiffness terms. The waveguide density, ρ_w, represents the inertia term for the extensional mode, whereas ρ_w and part of the shape factor, K, together form the inertia term for the torsional mode.

The shape factor, K, is proportional to the square root of the torsional rigidity constant, J, divided by the cross-section polar moment of inertia, I:[6]

$$K = \sqrt{\frac{J}{I}} . \quad (4)$$

For any arbitrary waveguide cross-section expressed in rectangular coordinates (x,y), the torsional rigidity constant, J, may be computed by

$$J = \iint F(x,y)\, dx\, dy , \quad (5)$$

where the integrations are taken over the cross-section and the function F(x,y) is equal to zero on the boundary of the cross-section and satisfies the nonhomogeneous Laplace equation,

$$\frac{\partial^2 F}{\partial x^2} + \frac{\partial^2 F}{\partial y^2} + 4 = o , \quad (6)$$

within the boundary.[7] The cross-section polar moment of inertia may be computed by

$$I = \iint (x^2 + y^2)\, dx\, dy \tag{7}$$

over the same region. For a waveguide of circular cross-section, K is equal to one; as the geometry departs from a circle, K becomes less than unity. Utilizing complex numerical methods, K was computed for several representative cross-section geometries. The cross-sectional area, A, polar moment of inertia, I, torsional rigidity constant, J, and shape constant, K, are listed in Table 1 for each geometry. The first three shapes are the unit circle, unit square, and unit equilateral triangle. The subsequent shapes each have 3/1 aspect ratios. The aspect ratio of a waveguide is defined as its greater cross-sectional dimension (width), divided by the equal or lesser orthogonal cross-sectional dimension (height).

For a waveguide completely immersed in a fluid of density ρ, the extensional propagation remains essentially unchanged, except for small attenuation losses. However, since the torsional motion of a noncircular waveguide is well coupled to the fluid, both energy and momentum are easily transferred to the fluid. The results are not only decreased velocity, but amplitude attenuation caused by the viscosity of the fluid as well. The fact that the waveguide cross-section is noncircular causes inertia from the surrounding fluid to be coupled to the waveguide, thus increasing the effective inertia of the waveguide. Clearly, from Equation 1, (page 8) the torsional wave velocity is

Table 1. Shape constants for representative waveguide cross-sectional geometries.

Shape	A	I	J	K
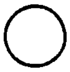	0.78	1.57	1.57	1.00
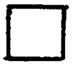	1.00	0.1667	0.1388	0.912
	0.433	0.0361	0.0214	0.770
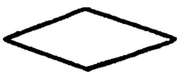	1.50	0.625	0.203	0.570
	2.79	2.05	0.649	0.563
	3.00	2.50	0.781	0.559
	1.50	0.646	0.191	0.544
	2.04	0.844	0.235	0.527
	2.17	1.23	0.280	0.477
	1.50	0.813	0.165	0.451

thereby decreased by a proportional amount. Drag is not present in rods of circular cross-section, thus, velocity is unaffected; however, the viscosity effects remain. These phenomena are incorporated into an expression by Lynnworth:[8]

$$v_t = K \sqrt{\frac{S}{\rho_w}} \left[1 + \frac{\rho}{2\rho_w} (1 - \frac{1}{K}) \right] . \tag{8}$$

Equation 8 was empirically determined by analysis of data resulting from experimental studies of the velocity of torsional acoustic waves in rectangular waveguides. However, laboratory tests at ORNL have shown that Equation 8 is not a generally valid expression of the torsional acoustic propagation in arbitrarily shaped waveguides, such as those listed in Table 1. Waveguides with nonrectangular cross-sections (triangle, semi-circle, and tear shapes) were fabricated and tested. The torsional velocity of propagation was measured for each of the waveguides and found to differ markedly from that predicted by Lynnworth's equation (Equation 8). Thus, any correct theoretical expression of the velocity of torsional acoustic propagation in arbitrarily shaped waveguides will be difficult to obtain, and probably involve solving nonlinear partial differential equations.

Temperature dependence of acoustic stress pulse velocity is realized by the temperature dependence of elastic moduli and density, as well as length, of the waveguide. An increase in temperature decreases both stiffness and inertia terms in Equation 1 (page 8). For stainless steel, the stiffness terms (S and Y) decrease at a rate approximately a factor of ten greater than the rate for the density term (ρ_w). This obviously results in a net decrease in velocity (or increase in transit time) with an increase in temperature for each acoustic wave transmission mode.

The characteristic impedances of an acoustic waveguide are represented by

$$Ze = \rho_w v_e A = A\sqrt{\rho_w Y}\ , \qquad (9)$$

for extensional waves, and by

$$Z_t = \rho_w v_t I = \sqrt{IJ\rho_w S}\ , \qquad (10)$$

for torsional waves, where A is the cross-sectional area of the waveguide. An impedance mismatch of adjacent sides at a boundary of the waveguide causes an incident wave to be partially reflected (and, obviously, partially transmitted) at the boundary. The well known reflection coefficient, Γ, is expressed by

$$\Gamma_{1,2} = \frac{Z_1 - Z_2}{Z_1 + Z_2}\ . \qquad (11)$$

Amplitude attenuation of an acoustic wave results from the partial transfer of the wave's energy to an adjacent medium, and from internal absorption losses. Laboratory tests have shown that a rectangular waveguide with 2/1 aspect ratio has an attenuation coefficient of 12% per meter.[9] Figure 5 is a graph of stress pulse amplitude (electrically speaking) vs transmission length. The data are shown fitted to a curve (solid line) with exponential decay. Deviations from this curve

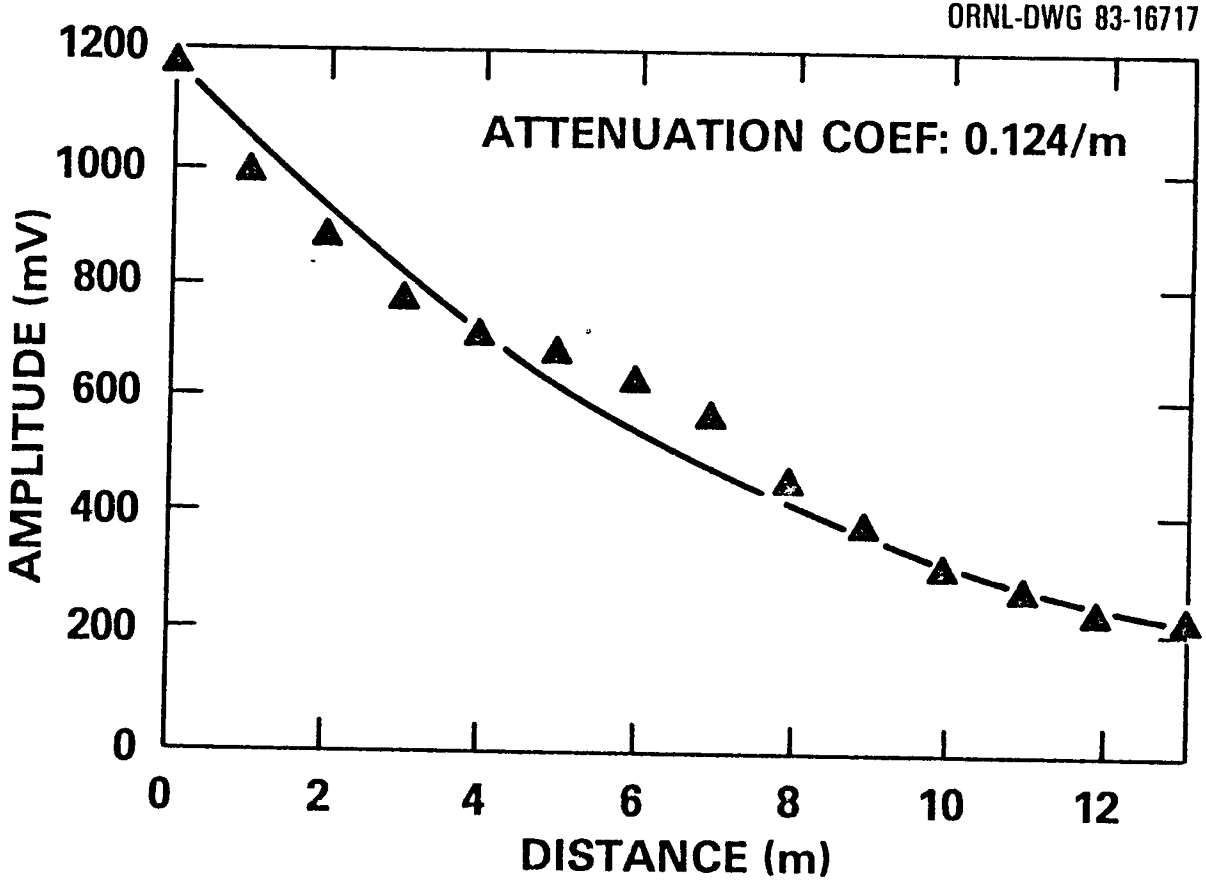

Figure 5. Amplitude attenuation as function of transmission length.

are probably due to the material and dimensional nonuniformities inherent in such lengthy waveguides. Similar tests of circular waveguides revealed an attenuation coefficient of 10% per meter.

A traveling acoustic wave pulse contains a broad, symmetrical spectrum of frequencies about a center frequency, f_o. The relationship that exists among the wavelength, λ, frequency, f, and velocity, v, of the traveling wave is expressed by

$$\lambda = \frac{v}{f} . \tag{12}$$

Dispersion, or the dependency of velocity on frequency, causes the pulse shape of the wave to spread out in time into many half cycles of pulse amplitude. For dispersionless propagation of the acoustic wave, the ratio of waveguide diameter (or width) to acoustic wavelength must be kept below a critical value.[10] Typically, this value is 1:8; hence, the expression, "thin waveguide." For maximum energy transfer and minimum dispersion, the magnetic coil transducer may be designed to have a length approximately one-half that of the acoustic stress-pulse wavelength.

Principle of Operation

The ultrasonic level probe and measurement system consists of a sensor, a transducer, signal conditioning electronics, and a data processor (see Figure 6). The sensor is a rectangular stainless steel rod which serves as an acoustic waveguide and is housed in a perforated tube. It is coupled to a transducer by a lead-in waveguide through a sensor/transducer boundary interface. The transducer consists of a

ORNL-DWG 83-16722

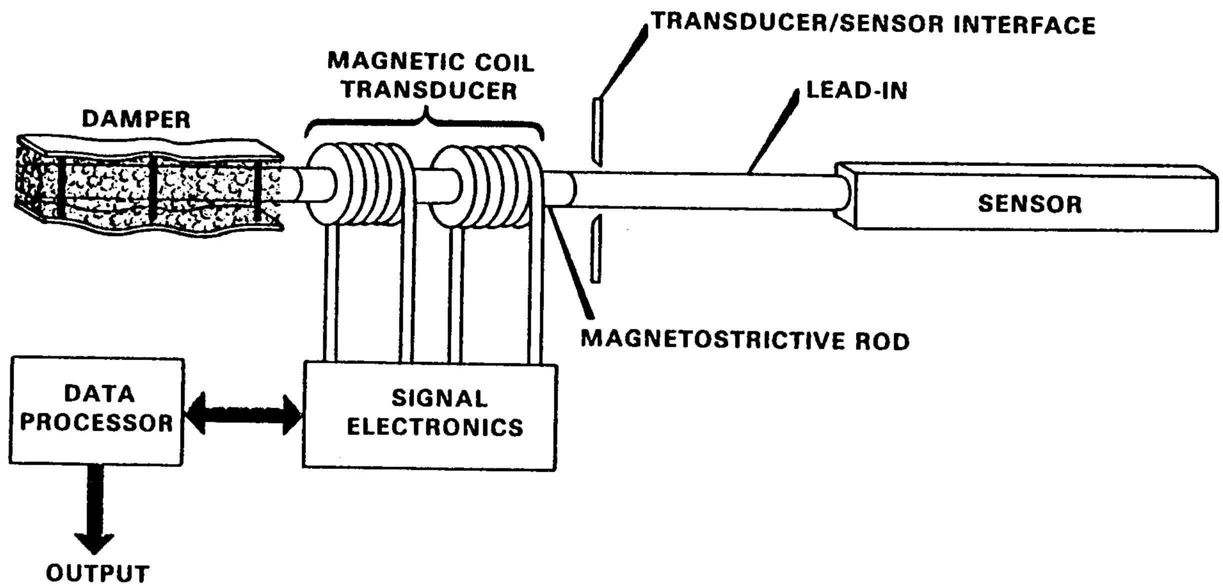

Figure 6. Components of level probe and measurement system.

1.6 mm-diam section of magnetostrictive material, such as remendur (composition 49 Co, 2-5 V, bal Fe; permanent magnet alloy with high curie temperature and high residual induction), linked by a pair of magnetic wire coils. The transducer is terminated by a back-length waveguide which is surrounded by the damper. The damper is, of course, the main subject of this thesis, and will be discussed in Chapters III and IV. The transducer coils are excited by the signal conditioning electronics which both transmits and receives the signal pulses to provide information to the data processor.

The transducer coils are magnetically biased in such a way that one coil produces extensional acoustic waves while the other produces torsional acoustic waves in the waveguide. The signal conditioning electronics provide current pulses up to 20 amperes with widths from 2 to 20 micro-seconds to each coil in an alternating sequence to launch extensional and torsional acoustic waves in the magnetostrictive rod in each direction. Transducer coils of 800 ampere-turns are sufficient to completely magnetically saturate the remendur. The acoustic waves traveling in the back-length section are absorbed by the damper so as not to be reflected back to the transducer from this end and interfere with the signals from the sensor. Forward launched acoustic stress pulses propagate in the waveguide through the sensor/transducer interface along the lead-in section to the sensor. Incident waves are partially reflected at the lead-in/sensor interface, at the sensor termination, and at any discontinuities used to divide the sensor into zones at measured intervals along its length. Reflected waves travel back to the transducer coils where they are converted to electrical signals (up to 2 volts peak-peak), received by the signal conditioning electronics, and utilized to measure the round-trip transit time of each wave in the sensor. A nominal value for extensional wave velocity of propagation is 5000 m/s at waveguide temperature of 25°C. The torsional velocity is less than or equal to this value, depending on the shape factor, temperature, and fluid density effects. For a rectangular waveguide which has a 2/1 aspect ratio and is immersed in water at a temperature of 25°C, the torsional wave velocity is approximately 3200 m/s.

The measured torsional wave transit time is a function of the density and temperature of the fluid surrounding the sensor. The measured extensional wave transit time is a function of the temperature component of the torsional wave signal only, and is used as a temperature compensation factor by the data processor to calculate fluid density, or level.

CHAPTER III

DAMPER DESIGN AND ANALYSIS

The requirement that acoustic stress pulse signals from the sensor be readily detectable and absent of spurious back-end wave reflections and prolonged ringing established the need for a means of eliminating interfering back-end acoustic waves from the waveguide. Previous alternatives included the utilization of a long back-length section to remove the back-end traveling acoustic waves in time, and rubber or fiberglass dampers; however, these solutions either compromised dimensional constraints of the probe, or had no chance of surviving nuclear reactor environments. Then, by strictly intuitive reasoning, the idea of constructing an all-metal damper which could endure the hostile environment of a reactor vessel was conceived by the author. An experimental stainless steel damper was subsequently designed, fabricated and tested. This chapter presents the design details of the damper, describes heuristically the damper mechanism, and concludes with an approximate mathematical model of the damper.

Physical Details

Figure 7 is an isometric view of a damper coupled to the back-length portion of an acoustic waveguide. The damper consists of a stainless steel wool surrounding a section of the waveguide in which acoustic stress pulse signals are to be damped. The wool which surrounds the waveguide is contained between two rigid stainless steel brackets which are formed with a sinusoidally bent pattern along their length. The bent pattern has a wavelength approximately equal to that

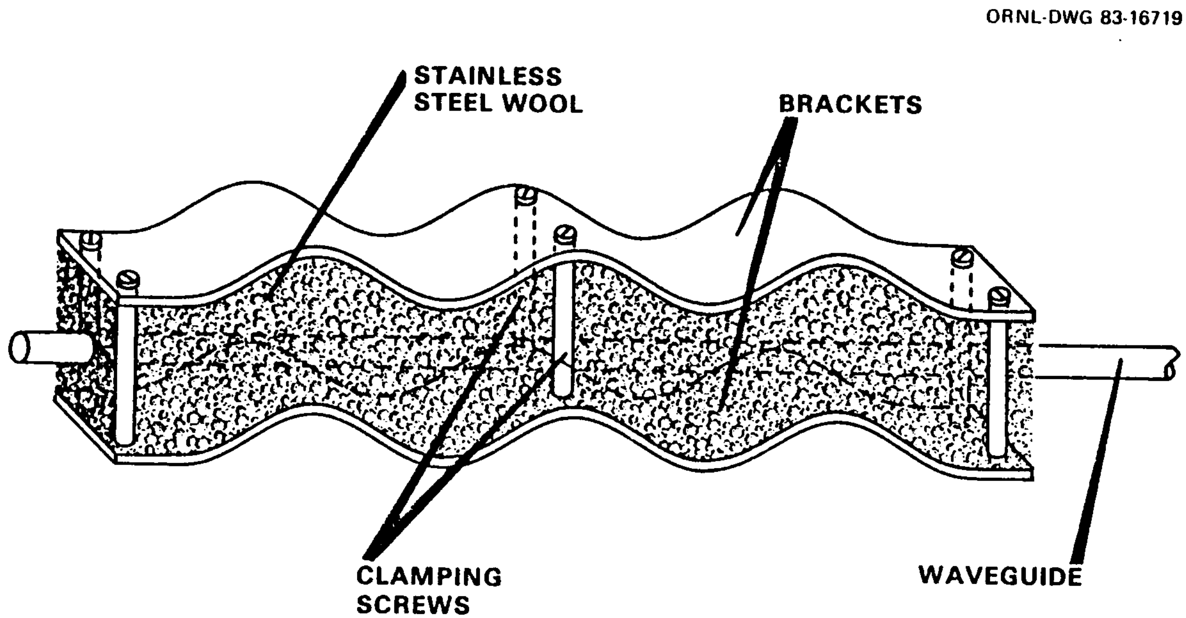

Figure 7. Damper design details.

of the acoustic signal to be damped. Although a sine wave pattern is illustrated here, other generally sinusoidal patterns which provide the proper forces may be employed. The bent pattern of the upper bracket is oriented in phase with the lower bracket pattern. A means, such as the clamping screws, is provided to force the plates toward each other and thereby compress the wool against the waveguide. This subjects the waveguide to alternately opposing lateral bending stresses at 180 degree intervals along its length in the area to be damped. The bent pattern also produces a pinching effect, and provides better coupling of the steel wool to the waveguide.

The experimental damper shown in Figure 8 was fabricated and applied to a waveguide with circular cross-section of 1.6 mm-diam. The damper brackets were 1.6 mm-thick plates 12.7 mm-wide by 203.2 mm in length. The bending pattern wavelength was about 25 mm, compared to the 30.5 mm wavelength of the acoustic waves to be damped. The bent pattern amplitude was about 6 mm peak-to-peak. The thickness of the steel wool mass surrounding the waveguide between the sinusoidal brackets prior to compression was about 25 mm. Chapter IV summarizes the experimental results of tests conducted on this damper.

Mechanism of Operation

With no damper present, recall that for an acoustic waveguide in a vacuum, the extensional mode and torsional mode acoustic wave velocity of propagation may be approximated by

$$V_e = \sqrt{\frac{Y}{\rho_w}} \quad , \tag{13}$$

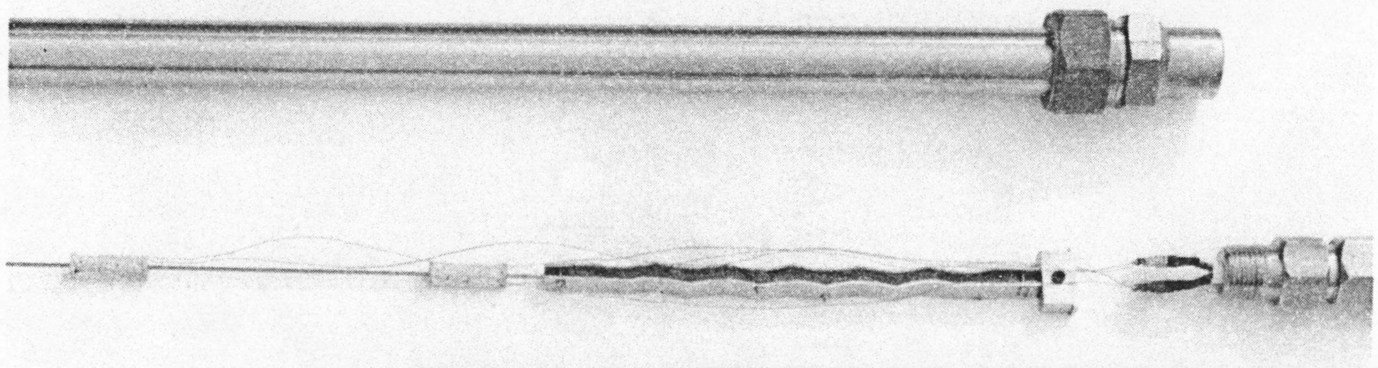

Figure 8. Photograph of damper installed on waveguide.

and,

$$V_t = K\sqrt{\frac{S}{\rho_w}} = \sqrt{\frac{JS}{I\rho_w}}\ . \tag{14}$$

These are equations for the velocities of propagation and do not reflect the slight attenuation experienced by such waves in practice. This attenuation is present, even for extensional mode propagation along a waveguide in a vacuum, due to almost negligible internal losses. When the waveguide is immersed in a viscous fluid, such as water, the attenuation becomes more noticable (10-12%/m) since additional energy is dissipated into the fluid as a result of the viscous friction between the waveguide and the fluid. In the case of torsional mode propagation along a noncircular waveguide immersed in a fluid, drag of the fluid opposes the torsional wave induced motion of the waveguide and effectively couples inertia from the fluid to the waveguide. The noncircular geometry aides in the transfer of momentum to the fluid as the apparent inertia of the waveguide, $I\rho_w$, is increased, thereby (Equation 14) decreasing the velocity of propagation, V_t.

The damper is applied to a circular section of the waveguide. Since this portion of the waveguide is circular, no drag is present, thus the velocity of propagation is unaffected. Except for the case in which the damper is overtuned, the damper causes no reflection of the incident wave; therefore, the damper does not appreciably alter the characteristic impedance of the waveguide. Also, laboratory tests have demonstrated that the general shape of the acoustic wave electrical representation is maintained while the wave's amplitude is diminished by the damper. The velocity of propagation and characteristic impedance, which are comprised of stiffness and inertia terms, are not affected by the damper because the damper is applied to a circular portion of the waveguide. The mechanism for altering wave velocity and waveguide impedance is drag, which is present only in noncircular waveguides. In circular waveguides, viscous friction is the only effect, and is the mechanism for acoustic wave amplitude attenuation. The damper, therefore, behaves much like a pure source of viscous friction which acts on the waveguide in such a way that energy of an acoustic wave propagating in this region is dissipated, resulting in amplitude attenuation, only. Viscous friction is supplied to the waveguide as the steel wool is compressed against the waveguide, causing the inhomogeneous, spring-like composition of the wool to rub against the waveguide. This effect is more readily obtained for the torsional mode since the damper/waveguide interaction is more direct than that for the extensional mode. In the torsional mode the waveguide motion is azmuthal; whereas, in the extensional mode the motion is both longitudinal and axial (by Poisson's effect), and less easily coupled to the wool.

Distributed System Analogy

The foregoing discussion of the damper mechanism reveals characteristics similar in nature to those of a distributed parameter, linear, distortionless transmission line of infinite length. Whereas the damper in reality is not an infinite distortionless waveguide, its properties may be approximated to resemble those of a distortionless transmission line, and the damper shall therefore be modeled as such.

Two essential steps are involved in the analysis of a physical system: the formulation of mathematical equations that describe the system in accordance with physical laws, and the solutions of these equations subject to appropriate initial or boundary conditions. In the formulation of equations that describe a physical system, emphasis is oriented toward electrical circuits, since they are easy to symbolize and construct, and special techniques have been developed to analyze them. Non-electrical systems, such as the damper, have electrical analogies because the equations that describe them are of the same form as those which describe the electrical circuits. Transmission lines and acoustic waveguides are examples of distributed parameter systems having component elements which are distributed in character, and are described by partial differential equations since more than one independent variable is involved; namely, time and space. This is in contrast to lumped parameter systems whose elements are lumped, and whose observables satisfy ordinary differential equations.

The classical distributed parameter electrical circuit model of a transmission line is shown in Figure 9. Letting

R = resistance per unit length,

L = inductance per unit length,

C = capacitance per unit length, and

G = leakage conductance per unit length,

we have

$$-\frac{\partial e}{\partial x} = Ri + L\frac{\partial i}{\partial t} \tag{15}$$

$$-\frac{\partial i}{\partial x} = Ge + C\frac{\partial e}{\partial t} \quad . \tag{16}$$

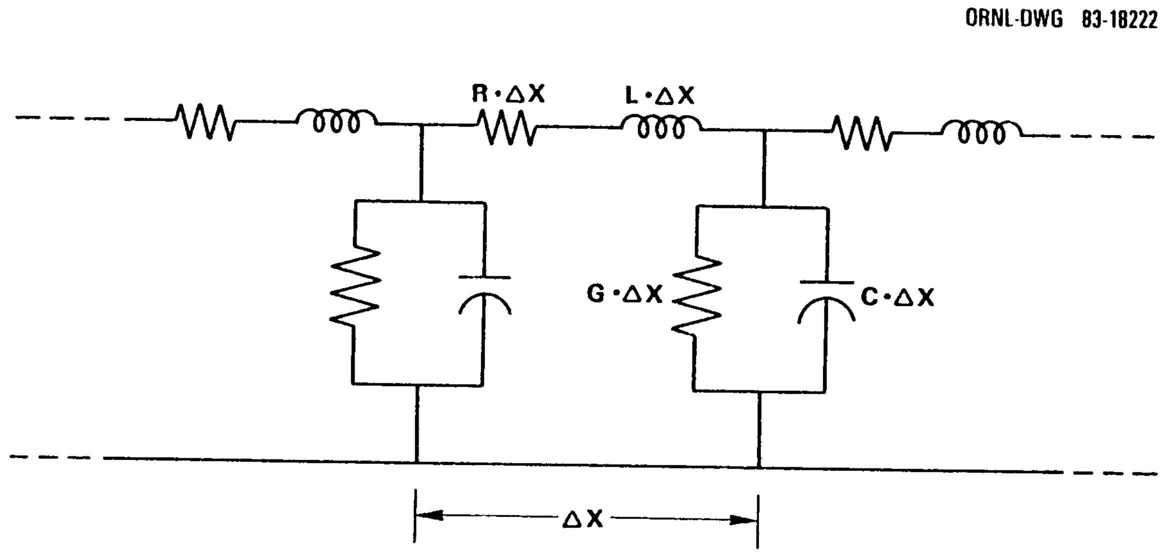

Figure 9. Distributed parameter representation of a transmission line.

Equations 15 and 16 (page 26) are called "transmission line equations," where $e = e(x,t)$ is the voltage drop per Δx, and $i = i(x,t)$ is the current decrease per Δx. The independent variable, x, is the distance measured from the sending end, whereas independent variable, t, corresponds to time. Differentiating Equation 15 (page 26) with respect to x, and Equation 16 (page 26) with respect to t, followed by some manipulation of the terms, results in the expression,

$$\frac{\partial^2 e}{\partial x^2} = LC\,\frac{\partial^2 e}{\partial t^2} + (RC + LG)\,\frac{\partial e}{\partial t} + RGe\ , \tag{17}$$

which is known as a "telegraphist's equation." One method for solving a partial differential equation, such as Equation 17, is to first convert it into an ordinary differential equation by the Laplace transformation, and then solve the latter by classical methods. Taking the Laplace transformation of Equation 17, the following is obtained:

$$\frac{d^2E(x,s)}{dx^2} - \gamma^2E(x,s) = L\,\frac{di(x,o)}{dx} - C(Ls + R)\ e(x,o)\ , \tag{18}$$

where,

$$\gamma = \sqrt{(Ls + R)(Cs + G)} \tag{19}$$

is the propagation constant.[11] Assuming zero initial conditions, $i(x,o) = e(x,o) = o$, Equation 18 reduces to

$$\frac{d^2E(x,s)}{dx^2} - \gamma^2E(x,s) = o\ , \tag{20}$$

which has the general solution

$$E(x,s) = A\,\varepsilon^{-\gamma x} + B\varepsilon^{\gamma x} \; . \qquad (21)$$

Since E(x,s) must remain finite even when x is infinite, it follows from Equation 21 that B = o. Now, let

$$f(t) = e(o,t) \qquad (22)$$

be the electrical representation of an acoustic wave introduced into a waveguide where x = o. Then, from Equation 21

$$A = E(o,s) = \mathcal{L}\{e(o,t)\} = \mathcal{L}\{F(t)\} = F(s) \; , \qquad (23)$$

and thus the solution to Equation 20 takes the form:[12]

$$E(x,s) = F(s)\varepsilon^{-\gamma x} \; . \qquad (24)$$

Approximating the acoustic waveguide without the damper by an analogous lossless transmission line, we have

$$R = G = o \; , \qquad (25)$$

and, from Equation 19,

$$\gamma = s\sqrt{LC} \; . \qquad (26)$$

Then, Equation 24 reduces to

$$E(x,s) = F(s)\varepsilon^{-sx\sqrt{LC}} \; , \qquad (27)$$

and the signal propagating in the waveguide may be modeled by

$$e(x,t) = f(t - x\sqrt{LC}) \ . \tag{28}$$

When the damper is applied to the waveguide, viscous friction is introduced which is analogous to adding lossy terms, R and G, to the transmission line of Figure 9 (page 27). Attenuation is the only noticeable effect that the damper has on the wave propagation; there is no change in the velocity of propagation (Equations 13 and 14 on pages 22 and 24), the characteristic impedance (Equations 9 and 10 on page 14) of the waveguide, nor in the shape of the traveling waveform. Clearly, the inertia and stiffness terms, L and C, are not appreciably altered. However, R and G must obey a special relationship if the model is to include the characteristic that the traveling wave's shape is maintained. The acoustic waveguide and damper may thus be approximated by an analogous distortionless transmission line, where

$$\frac{R}{G} = \frac{L}{C} \ . \tag{29}$$

Then, Equation 19 (page 28) becomes

$$\gamma = \sqrt{RG} + s\sqrt{LC} \ , \tag{30}$$

and Equation 24 reduces to

$$E(x,s) = F(s)\varepsilon^{-x\sqrt{RG}} \ \varepsilon^{-sx\sqrt{LC}} \ . \tag{31}$$

Therefore, the signal propagating in the region of the waveguide surrounded by the damper may be modeled by

$$e(x,t) = \varepsilon^{-x\sqrt{RG}} f(t - x\sqrt{LC}) , \tag{32}$$

where $x = o$ is the point along the waveguide at which the traveling wave, $f(t - x\sqrt{LC})$, enters the damper. The term, $\sqrt{RG}$, is called the attenuation constant, and is proportional to the amount of viscous friction and internal losses supplied by the damper, causing the otherwise unchanged signal to exponentially decay as it travels over the length of the damper. For values of $x\sqrt{RG} \geq 4$, the amplitude of $e(x,t)$ in Equation 32 is more than 98% attenuated.

Table 2 is a comparison of analogous equations, expressions, and parameters that exist relative to the electrical transmission line, acoustic extensional wave propagation in an elastic bar, and torsional wave propagation in a rod of circular cross-section.

Table 2. Comparison of analogous systems

EXPRESSION	ELECTRICAL	EXTENSIONAL	TORSIONAL
WAVE EQUATION (LOSSLESS CASE)	$\frac{\partial^2 e}{\partial x^2} = \frac{1}{v^2}\frac{\partial^2 e}{\partial t^2}$	$\frac{\partial^2 E}{\partial x^2} = \frac{1}{v^2}\frac{\partial^2 E}{\partial x^2}$	$\frac{\partial^2 \theta}{\partial x^2} = \frac{1}{v^2}\frac{\partial^2 \theta}{\partial t^2}$
VELOCITY OF PROPAGATION, v	$\frac{1}{\sqrt{LC}}$	$\sqrt{\frac{Y}{\rho_w}}$	$\sqrt{\frac{S}{\rho_w}}$
CHARACTERISTIC IMPEDANCE, Z_o	$\sqrt{\frac{L}{C}}$	$A\sqrt{\rho_w Y}$	$\sqrt{IJ\rho_w S}$
ATTENUATION CONSTANT	$\sqrt{RG}$	$\sqrt{\frac{D_e}{f_e}}$	$\sqrt{\frac{D_t}{f_t}}$
INERTIA TERM	L	ρ_w	ρ_w
STIFFNESS TERM	$\frac{1}{C}$	Y	S

where, E = longitudinal displacement from the equilibrium position of the elastic bar,

θ = angular displacement from the equilibrium position of the rod of circular cross-section ($k = \sqrt{\frac{J}{I}} = 1$),

D_e, f_e = lossy terms supplied by damper for extensional mode, and

D_t, f_t = lossy terms supplied by the damper for torsional mode.

CHAPTER IV

EXPERIMENTAL RESULTS

The prototypic damper shown in Figure 8 (page 23) was designed, fabricated, and installed on an acoustic waveguide. Tests were conducted in which acoustic waves of different modes were introduced into the waveguide and allowed to pass into the damper. The effects on these signals of tuning the damper to various degrees were observed and recorded. This chapter describes the test configuration and procedures, and then presents the results.

Test Configuration and Procedures

Figure 10 is a block diagram of the configuration set up for the tests. The waveguide consists of a section of 1 mm × 2 mm stainless steel ribbon (sensor) welded to a 1.6 mm-diam stainless steel rod (lead-in), whose other end is welded to a 1.6 mm-diam section of remendur. Two magnetic coils surround the remendur to form the transducer, approximately 70 cm from point c (lead-in/sensor interface). A 1.6 mm-diam stainless steel rod (back-length) is attached to the remendur to provide support for the damper. The coils are connected to a Panametrics Panatherm 5010C Ultrasonic Profiler (pulser/receiver) whose output is monitored on an oscilloscope and recorded by means of a Polaroid camera. A deep-discharge, 12 VDC, wet-cell battery provides the current necessary to establish the azimuthal bias in the remendur for generating torsional stress pulses; a permanent magnet removes this bias such that extensional stress pulses may be generated in one of the two coils. In a modified test configuration (Figure 11), the

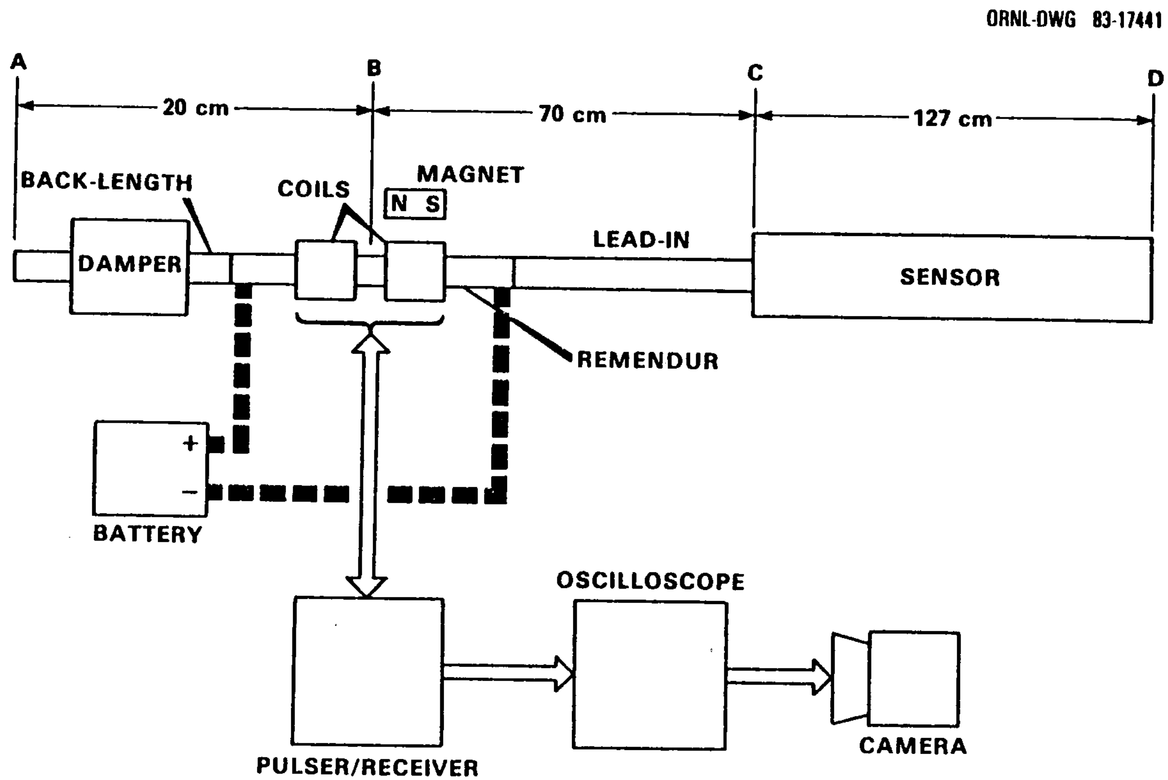

Figure 10. Test configuration block diagram.

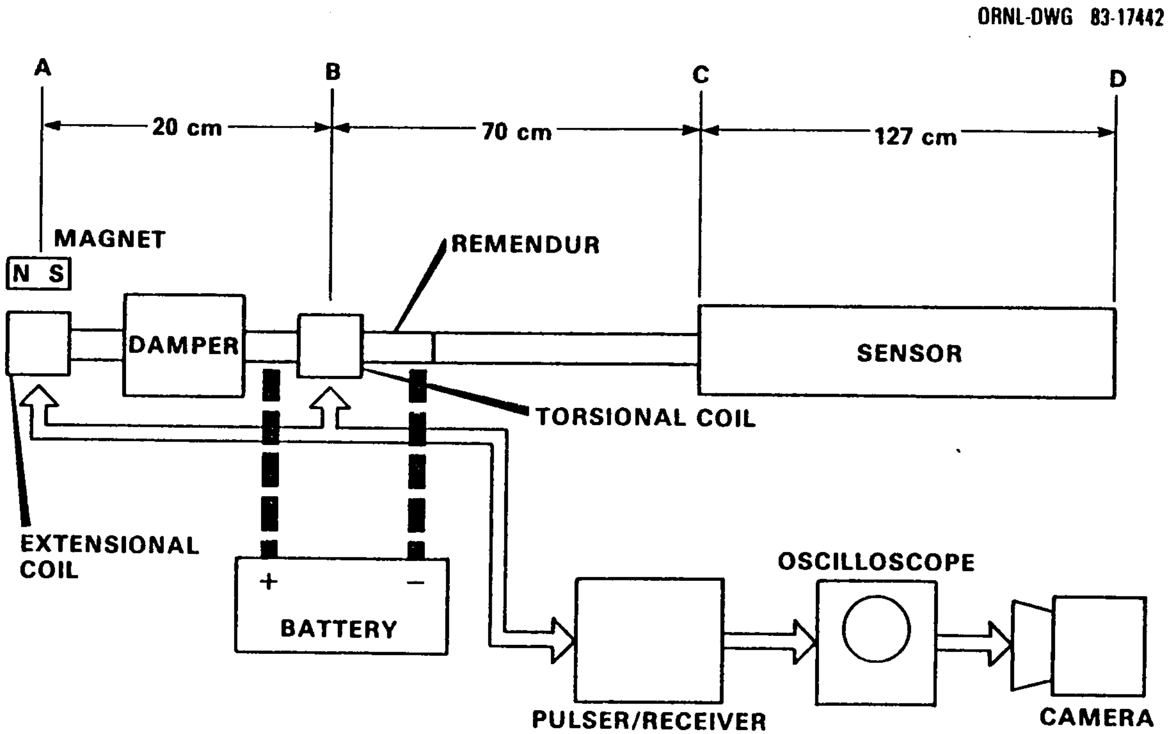

Figure 11. Modified test configuration with damper between extensional and torsional coils.

extensional coil is placed at the back end of the waveguide, followed by the damper and the torsional coil. This configuration extends the remendur rod to include the back-length section; the remaining configuration is the same as that shown in Figure 10 (page 34).

The Panatherm 5010C pulser/receiver is programmed to first pulse a selected coil, launching an acoustic wave into the waveguide, and then receive and amplify the signal produced by the coil as reflected acoustic waves return to the coil. In this way, each coil is excited in an alternating sequence, and the resulting waveforms (electrical representations of reflected acoustic stress pulses) are displayed on the oscilloscope. Additionally, a sync pulse is provided by the pulser/receiver which toggles high/low on alternating pulses to indicate which signal mode, torsional or extensional, is present at the output. This sync output is utilized at the oscilloscope's trigger input in such a way that the user may selectively monitor either signal mode by adjusting the negative/positive trigger level switch on the oscilloscope.

The torsional mode was selected for viewing while the damper was tuned. Oscillograms of the torsional mode waveform were taken by the camera before the damper was applied and after the damper was tuned to absorb the torsional back-end reflections. Tuning is accomplished by progressively tightening the clamping screws on the damper, while observing the selected waveform, until the back-end reflections' amplitude is reduced to a minimum. Excessive tuning after the minimum is reached may cause the traveling acoustic stress pulses to be reflected by the damper itself. This procedure was similarly repeated for the extensional mode.

Next, the damper was tuned to eliminate extensional waves, but the torsional mode waveform was recorded. Then, the extensional mode signals were recorded while the damper was tuned to remove the torsional back-end reflections.

Finally, the modified test configuration in Figure 11 (page 35) was implemented, and the damper was tuned to absorb torsional waves. This arrangement allowed extensional mode stress pulses to pass through the damper and travel on to the sensor, while the damper absorbed torsional mode stress pulses. There were no extensional back-end reflections since there was no back-length section behind the extensional coil.

System Performance

The oscillograms resulting from the aforementioned tests are reproduced on pages to follow. Figure 12 represents the torsional mode signals present in the waveguide without the damper in use. The voltage spikes are known as echoes, and represent traveling acoustic stress pulses which have been reflected at discontinuities along the waveguide and have subsequently propagated back to the originating coil. Echoes α and β (Figure 12) are the signals of interest which were reflected at points c and d (Figure 10 on page 34), respectively, from the sensor boundaries. The other echoes in Figure 12 are the undesirable reflections from the back-end of the waveguide. Figure 13 is the same torsional signal except that the damper was tuned to eliminate the back-end echoes. Note that only the desired signals from the sensor, echoes α and β, are present. Similar results for the extensional mode are found in Figures 14 and 15. Figure 14 shows noise corrupted

ORNL-DWG 83-17445

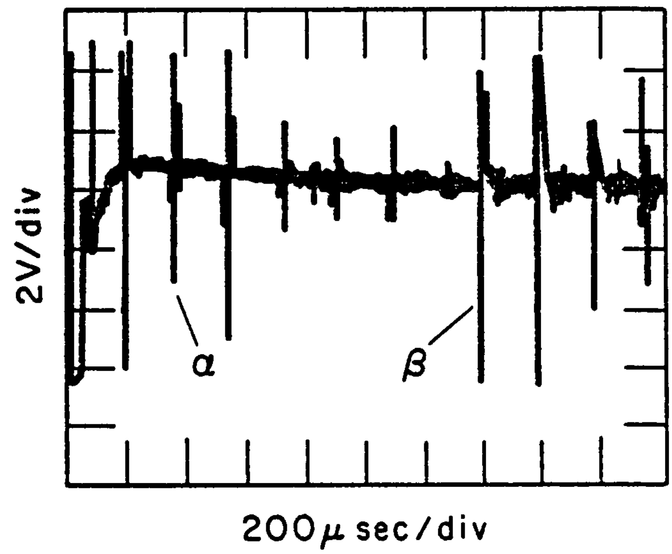

Figure 12. Torsional signal with no damper applied.

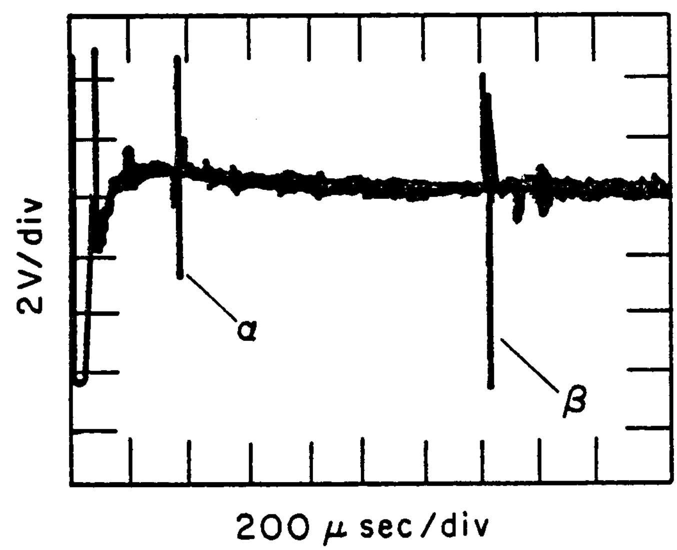

Figure 13. Torsional signal with damper tuned for torsional mode.

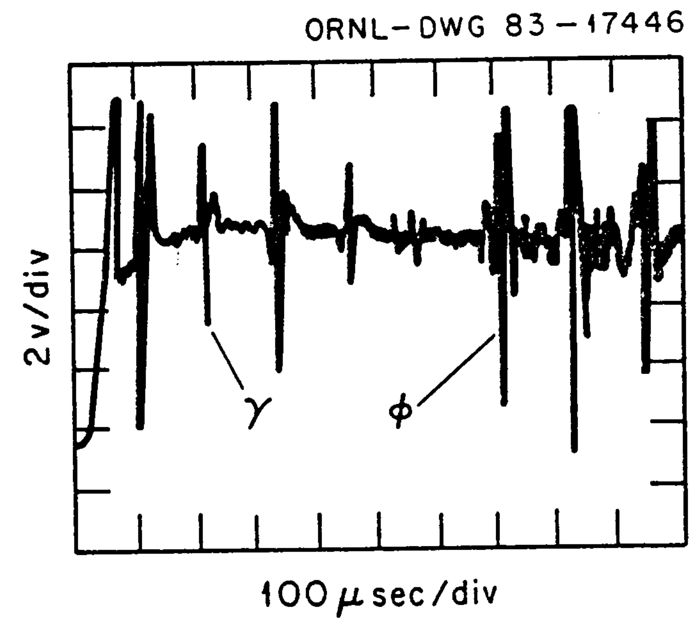

Figure 14. Extensional signal with no damper applied.

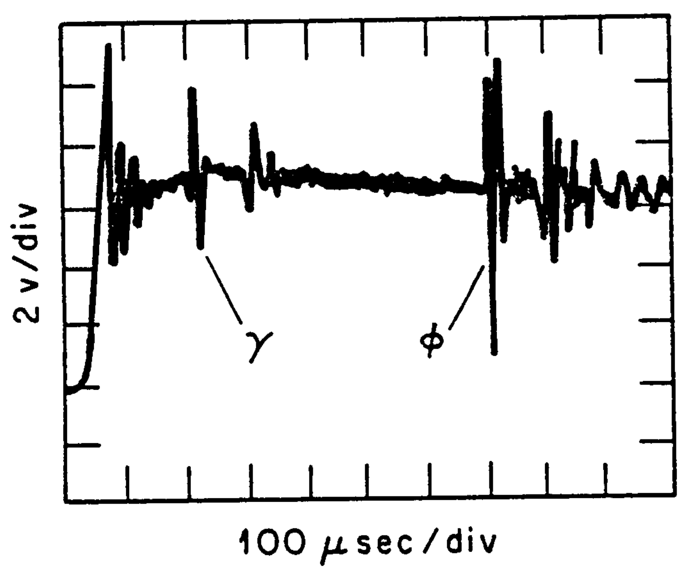

Figure 15. Extensional signal with damper tuned for extensional mode.

extensional mode echoes with no damper applied, whereas only signal echoes γ and ϕ, from points c and d, respectively, are dominant in Figure 15 after tuning the damper. Elimination of the extensional mode back-end echoes required additional tightening of the damper clamps as compared to that required for the torsional mode. With the damper tuned for the extensional mode, the torsional mode waveform was re-examined. As can be seen in Figure 16, the torsional back-end reflections remain damped. By contrast, when the damper is tuned to eliminate torsional mode reflections, extensional mode back-end echoes are only slightly damped (see Figure 17). Thus, by this example it is possible to tune the damper to filter torsional stress pulses while allowing extensional stress pulses to pass. However, additional damping is required to absorb extensional stress pulses, and the torsional mode signals are simultaneously absorbed. With these ideas in mind, the test configuration was modified (refer to Figure 11 on page 35) to take advantage of selective filtering. With the extensional coil on the back-end of the waveguide, no back-end reflections are in a position to interfere; furthermore, forward launched extensional stress pulses pass through the damper tuned for the torsional mode, whereas torsional mode stress pulses traveling in the back-length are absorbed by the damper. The results of this configuration are shown in Figures 18 (torsional signals α and β) and 19 (extensional signals γ and ϕ). This method produces very clean signals in both modes, thereby optimizing dual-mode performance. This is the preferred method of operation, and has produced good results in practice with a working measurement system.

ORNL-DWG 83-17444

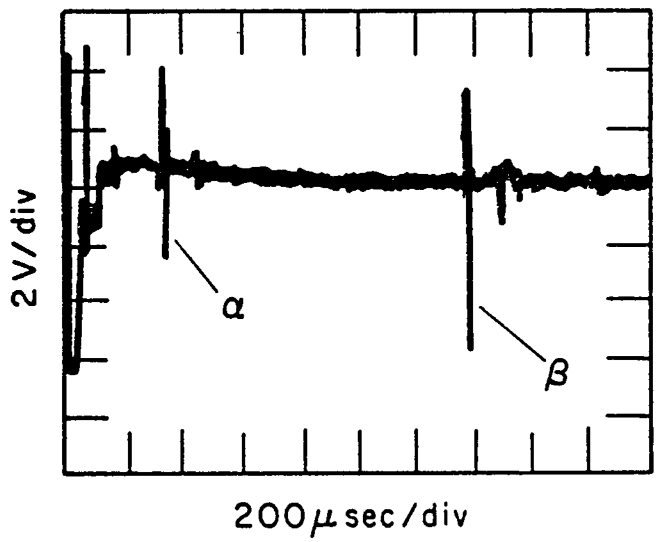

Figure 16. Torsional signal with damper tuned for extensional mode.

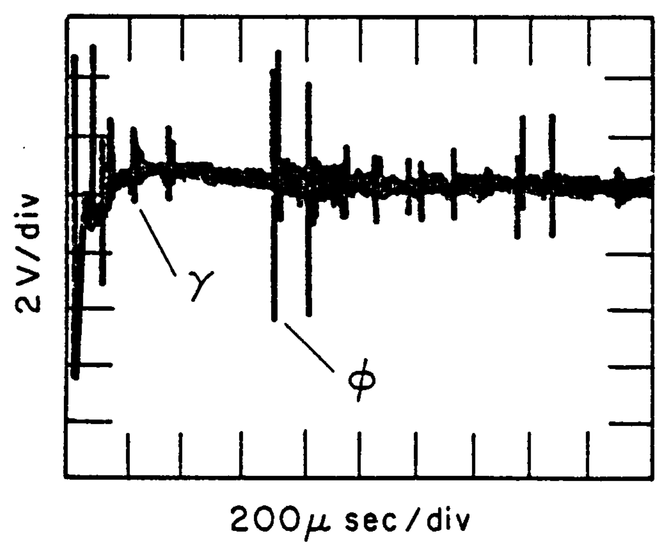

Figure 17. Extensional signal with damper tuned for torsional mode.

ORNL-DWG 83-17443

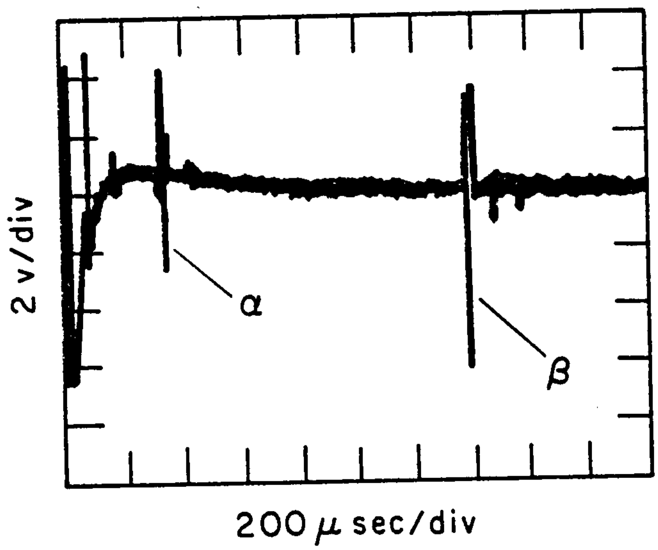

Figure 18. Torsional signal for modified configuration.

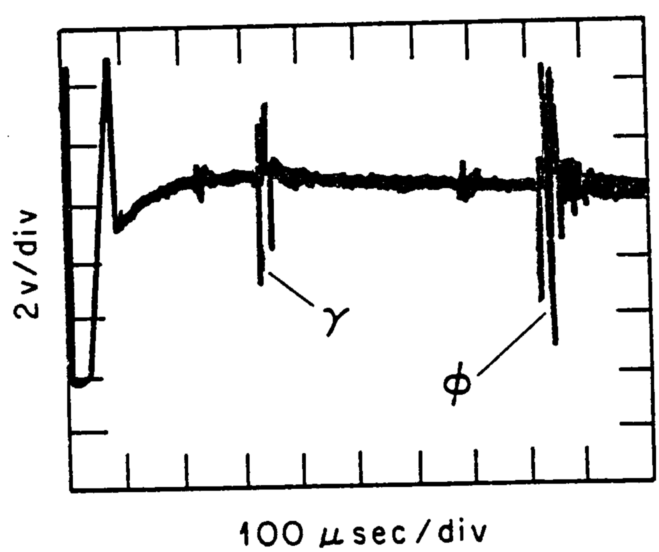

Figure 19. Extensional signal for modified configuration.

CHAPTER V

SUMMARY

A damper which removes undesirable stress pulses from an acoustic waveguide was successfully designed, constructed, and experimentally verified. A mathematical model was then developed to describe the damper's behavior in terms of an analogous distributed parameter transmission line. The damper serves to simplify the design and improve the performance of an ultrasonic water level measurement system. It is a by-product of research conducted at Oak Ridge National Laboratory to develop advanced instrumentation for use in pressurized water reactors.

The damper possesses salient features which contribute to its uniqueness. The damper is constructed entirely of stainless steel, and is capable of surviving a nuclear reactor environment. Previous state-of-the-art designs utilized materials which would fail under such conditions. The damper is tunable, an attribute which increases its flexibility for use in other more general applications. A simple design makes the damper easy to construct, and its self-contained, compact structure allows the damper to be applied as an integral part of the acoustic waveguide.

Acoustic stress pulses which propagate along the back-length section of the waveguide and enter the damper are completely attenuated. In this way, back-end reflections of the acoustic waves are prevented from interfering with signals received from the sensor portion of the waveguide, thus simplifying the pulse-echo discriminating electronics. Reverberations of acoustic waves with the back-end are likewise eliminated, greatly reducing the ringing effect and thereby increasing the upper limit of the transducer excitation repitation rate. This increases the rate at which signal information is gathered, extending the instruments bandwidth, improving correlation between torsional and extension modes, and sharpening resolution. Utilizing a damper rather than simply extending the back-length section reduces the probe length by greater than a factor of two, which will facilitate installation by keeping the probe within dimensional constraints of current reactor designs.

LIST OF REFERENCES

LIST OF REFERENCES

1. TMI-2 Lessons Learned Task Force Status Report and Short Term Recommendation, NUREG-0578, pp. A-11-12 (July 1979).

2. S. C. Rogers, G. N. Miller, IEEE Transactions on Nuclear Science, Vol. NS-29, No. 1, pp. 665-668 (February 1982).

3. G. N. Miller, R. L. Anderson, S. C. Rogers, et al., IEEE Ultrasonic Symposium Proc., Vol. 2, Cat. #80CH1602-2, pp. 877-881 (October 1980).

4. N. S. Tsannes, IEEE Transactions on Sonics and Ultrasonics, Vol. SU-13, No. 2, pp. 33-41 (July 1966).

5. R. M. Bozorth, Ferromagnetism, D. Van Nostrand Company, Inc., New York (1951).

6. S. Spinner and R. C. Valore, J. Natl. Bur. Std., Vol. 60, No. 5, Research Paper 2861 (May 1958).

7. G. Pickett, "Equations for Computing Elastic Constants from Flexural and Torsional Resonant Frequencies of Vibration of Prisms and Cylinders," Am. Soc. Test. Mater. Proc., Vol. 45, p. 846 (1945).

8. L. C. Lynnworth, IEEE Ultrasonics Symposium Proc., Cat. No. 77CH1264-ISU, pp. 29-34 (1977).

9. W. B. Dress, "A Torsional Ultrasonic Technique for LWR Liquid Level Measurement," NUREG/CR-3113, ORNL/TM-8585, pp. 2-3 (January 1983).

10. S. Davidson, "Wire and Strip Delay Lines," Ultrasonics (July-September 1966).

11. D. K. Cheng, Analysis of Linear Systems, Addison-Wesley Publishing Company, Inc., Reading, Massachusetts (1959).

12. Stanford Goldman, Transformation Calculus and Electrical Transients, Prentice-Hall, Inc., Englewood Cliffs, N.J. (1949).

VITA

Samuel C. Rogers was born on October 19, 1956, in Greenville, Alabama. The son of Kenneth C. and Pauline Dale Rogers, he was raised in Montgomery, Alabama, where he graduated from Sidney Lanier High School in 1975. He then attended Auburn University where in December of 1979 he received a Bachelor of Electrical Engineering degree with high honors. He entered the Graduate School at the University of Tennessee in the spring of 1980, and received his Master of Science degree with a major in Electrical Engineering in the fall of 1983. He is a member of National Honor Societies Phi Kappa Phi, Tau Beta Pi, Eta Kappa Nu, and Pi Mu Epsilon.

While in undergraduate school, Rogers worked as a Cooperative Education student at Southern Company Services, Inc. A Development Engineer with Union Carbide Corporation at the Oak Ridge National Laboratory since January of 1980, his responsibilities have included advanced instrumentation research and development, and process measurement and controls design. He has co-authored several technical papers which have been published in open literature, and is singularly named as inventor of "A Tunable Damper for an Acoustic Waveguide," for which a patent is pending. Rogers was a co-recipient of an IR-100 Award in 1982 for one of the year's 100 most significant technological advances, "Reactor Core Cooling Measurement System."